

High Speed Hazard Avoidance for Mobile Robots in Rough Terrain

Matthew Spenko*, Karl Iagnemma, Steven Dubowsky
Massachusetts Institute of Technology, 77 Massachusetts Avenue, Rm 3-469
Cambridge, MA USA 02139

ABSTRACT

Mobile robots have important applications in high speed, rough-terrain scenarios. In these scenarios, unexpected and hazardous situations can occur that require rapid hazard avoidance maneuvers. At high speeds, there is limited time to perform re-planning based on detailed vehicle and terrain models. Furthermore, detailed models often do not accurately predict the robot's performance due to model parameter and sensor uncertainty. This paper presents a method for high speed hazard avoidance. The method is based on the concept of the trajectory space, which is a compact model-based representation of a robot's dynamic performance limits in uneven, natural terrain. A Monte Carlo method for analyzing system performance despite model parameter uncertainty is briefly presented, and its integration with the trajectory space is discussed. Simulation results for the hazard avoidance algorithm are presented and demonstrate the effectiveness of the method.

Keywords: trajectory space, unmanned ground vehicles, autonomous robots, hazard avoidance, rough terrain

1 INTRODUCTION

Unmanned ground vehicles (UGVs) have important military, reconnaissance, and materials handling applications.^{1,2} Many of these applications require a UGV to move at high speeds through uneven, natural terrain with various compositions and physical parameters.

Often a UGV is directed to follow a pre-planned path (or navigate through pre-defined waypoints) designated by an off-line mission-level planning algorithm. However, in rough terrain at high speeds, it is likely that dangerous and unforeseen situations will occur that are not foreseen by the high-level planning methods. These may be the result of outdated topographical data, unidentified obstacles due to sensor limitations or errors, or unanticipated physical terrain conditions. In these situations a UGV must quickly execute a maneuver that allows it to safely avoid the impending hazard. Despite powerful on-board computers, at high speeds there is little time to perform re-planning based on detailed vehicle and terrain models. Furthermore, it is difficult to accurately model complex vehicle/terrain interactions due to uncertainty about the exact profile and nature of the terrain.

This paper presents a method for high speed hazard avoidance. It introduces the concept of the trajectory space, which is a compact framework for analyzing a UGV's dynamic performance on uneven, natural terrain. The trajectory space defines the performance limits of a UGV based on known or estimated vehicle parameters, terrain parameters, and hazard (obstacle) properties. This paper also briefly discusses a Monte Carlo method for analyzing system performance in spite of model parameter uncertainty, and its integration with the trajectory space. The effectiveness of the hazard avoidance technique is demonstrated through simulation results of a small UGV moving at high speeds through rough terrain.

2 BACKGROUND AND LITERATURE REVIEW

Hazard avoidance has traditionally been performed either by selecting from a set of predetermined paths (i.e. search techniques over small spaces), or by reactive (reflexive) behaviors, which evoke a pre-determined action in response to specific sensor signals. Many of these techniques have been designed for use on flat or slightly rolling terrain, at speeds

*mspenko@mit.edu; phone 1 617 253 2334; fax 1 617 258 7881; robots.mit.edu/people/mspenko

that do not excite vehicle dynamics.³⁻⁸ Here we address the problem of hazard avoidance on rough, uneven terrain at speeds that excite the vehicle's dynamics.

Researchers have developed a search-based technique to navigate a HMMWV-class vehicle at speeds up to 10 m/s while avoiding large obstacles.³ The method relies on a pre-computed database of approximately 15 million 20 to 30 meter long clothoid trajectories. Since the vehicle is assumed to travel on relatively flat terrain at fairly low speeds, the model used in the calculations does not consider vehicle dynamics. An online algorithm eliminates candidate clothoids that intersect with obstacles or are not feasible given the initial steering conditions. From the remaining paths, the algorithm chooses one that follows the most benign terrain. Computation time is ~250 msec, which suggests that with advances in computation power this technique could be applied to higher-speed situations. Also, vehicle dynamics could be incorporated into the algorithm by employing more complex vehicle models. However, the technique does not consider the important aspects of terrain roughness, inclination, and vehicle/terrain traction characteristics.

Researchers at Hughes Corporation have developed a fuzzy logic-based algorithm for reactive outdoor hazard avoidance.^{4,5} The approach arbitrates between hazard avoidance and goal seeking and allows for UGV navigation at speeds up to 1 m/s. Another successful reactive behavior-based technique was developed at Carnegie Mellon.⁶ In this case the "behaviors" are candidate steering angles, and an arbitrator chooses a steering angle based on obstacle and goal locations. Other work in the area has focused on problems arising from partially known and dynamic environments⁷ or sensing issues in outdoor terrains.⁸ Although these techniques have been successful at low to moderate speeds, they do not explicitly consider vehicle dynamics and changing terrain characteristics. Failure to consider these effects can result in trajectories that are impossible for a UGV to safely execute.

Recently, a locally randomized path planning technique has been proposed that attempts to address robot/terrain dynamics in real time.⁹ Randomized planning techniques are used to address the problems associated with real time operation and high dimensionality. Since its performance has not yet been fully documented, definite conclusions about this work cannot be drawn.

In this paper a hazard avoidance method is proposed that considers vehicle dynamics, terrain parameters, and hazard properties. It is computationally efficient enough for high-speed applications. The method is inspired by the work of Frazzoli in autonomous helicopter control, which draws on a library of pre-computed maneuvers to dynamically transition a vehicle from one stable motion trajectory to another.¹⁰ The technique described here incorporates features that are critical to UGV navigation, such as vehicle/terrain interaction, the presence of hazards, and terrain roughness and unevenness.

3 PROBLEM STATEMENT AND ASSUMPTIONS

Here we address the problem of UGV hazard avoidance at high speeds in rough terrain. "High speed" is loosely defined as speeds that excite the vehicle's dynamics and cause phenomena such as wheel slip, sideslip, tip-over, and ballistic behavior. Terrain roughness is defined as random or near-random unevenness with features on the order of one-half the vehicle wheel radius. Hazards are defined as discrete objects or terrain features greater than one-half the vehicle wheel radius, such as trees, boulders, ditches, hillocks, and knolls or any area of poorly traversable terrain (i.e. non-geometric hazards such as water or very soft soil). The UGV is assumed to be following a pre-planned path or navigating between pre-planned waypoints. The algorithm must rapidly plan a maneuver that causes the UGV to avoid an unexpected hazard while considering vehicle dynamics, vehicle/terrain interaction, and the performance limits of the vehicle.

Here we consider wheeled vehicles. We describe a terrain region by its average roll (ϕ), pitch (ψ), roughness (ϖ), and traction coefficient (μ). It is assumed that coarse estimates of the ground/tire traction coefficient and ground roughness are known or can be determined online. Techniques for measuring or estimating the above parameters are described

elsewhere.^{11,12,13} It is also assumed that vehicle inertial and kinematic properties are known with reasonable uncertainty. The vehicle is assumed to be equipped with the following sensors:

- A range sensor for measuring terrain elevation and locating hazards within 20 vehicle lengths;
- An inertial navigation sensor that can measure the vehicle’s roll, pitch, yaw, roll rates, pitch rates, yaw rates, and translational accelerations with reasonable uncertainty;
- A global positioning system sensor that can measure the vehicle’s position and velocity in space with reasonable uncertainty.

4 THE TRAJECTORY SPACE

The proposed hazard avoidance algorithm is based on the concept of the trajectory space, which is the space of a vehicle’s instantaneous curvature, ρ , and velocity, v . Constraints can be placed on the space to yield a compact representation of a vehicle’s performance limits over uneven terrain. Figure 1 shows an illustration of the trajectory space along with icons depicting a vehicle’s actions corresponding to various points in the space.

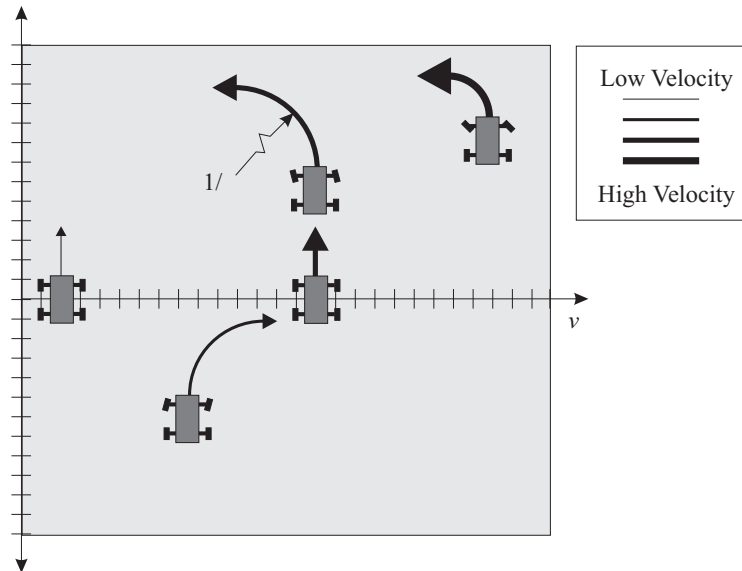


Figure 1: Representation of vehicle action as described by its location in the trajectory space.

The icon on the left shows a vehicle traveling straight (zero curvature) at a low speed. The icon at the upper right represents a vehicle turning sharply at high speed. Velocities are limited to positive values in this work.

4.1 The Admissible Trajectory Space

The Admissible Trajectory Space (ATS), N , is the portion of the trajectory space that a vehicle can safely maintain on a given terrain. Safe traversal by a UGV is defined by avoidance of roll-over and excessive sideslip. Boundaries of N are affected by steering mechanism and power train characteristics, terrain parameters, and vehicle kinematics and inertial parameters. Below is a description of ATS computation using simple models. Note that these simple models do not capture complex vehicle dynamics and vehicle/terrain interactions. In practice, offline dynamic simulations using high-order vehicle models and nonlinear vehicle/terrain interaction models are used to compute N .

4.2 Steering Mechanism and Power Train Limits

Most UGV steering mechanisms possess mechanical stops that limit the steering angle (see Figure 2).

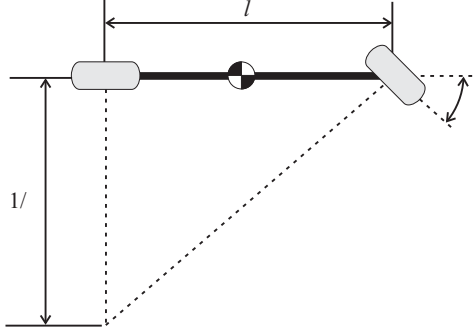


Figure 2: Top view of a “single-track” vehicle model used for steering mechanism limit computation.

Let A be the set of attainable curvatures for a vehicle based on steering mechanism limitations:

$$A \equiv \left\{ \forall \rho \mid |\rho| \leq \frac{l}{\tan \delta_{\max}} \right\} \quad (1)$$

where δ_{\max} is the maximum steering angle and l is the distance between the front and rear axles.

The power train consists of the vehicle engine and transmission. Power train output characteristics restrict the velocity of the vehicle. Let B be the set of allowable velocities for the vehicle based on power train limits:

$$B(\phi, \psi, \varpi, \mu) \equiv \{ \forall v \mid 0 \leq v \leq v_{\max}(\phi, \psi, \varpi, \mu) \} \quad (2)$$

where v_{\max} is the maximum vehicle velocity. Note that power train limits are a function of the terrain inclination and physical parameters.

4.3 Sideslip and Roll-Over Limits

The velocity and curvature pair at which a UGV will roll-over or exhibit sideslip are functions of the terrain parameters and the vehicle kinematic and inertial properties. Although some sideslip is expected and unavoidable, substantial slip that causes large heading or path following errors is detrimental. Roll-over is also generally undesirable despite the fact that some UGVs are designed to be invertible.¹ Slip limits can be computed from the free body diagram shown in Figure 3 assuming that $\dot{v} = 0$ and $\dot{\rho} = 0$. Here $\{xyz\}$ represents a body-fixed coordinate frame and $\{XYZ\}$ represents an inertial frame.

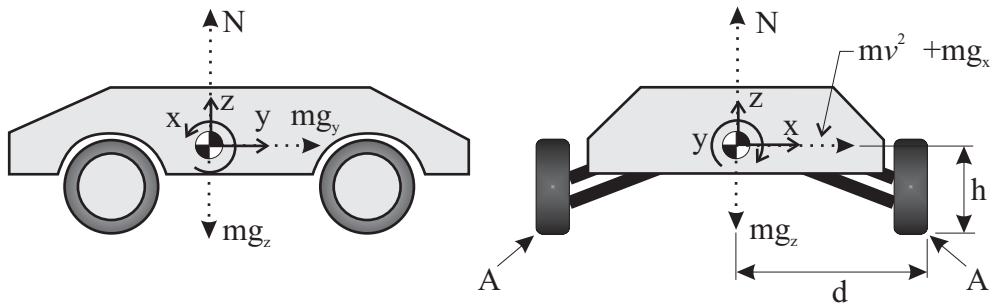


Figure 3: Free body diagram of a UGV.

For simplicity we assume the vehicle roll and pitch are equal to the terrain roll and pitch. The vehicle roll (ϕ), pitch (ψ), and yaw (θ) associated transformation matrices are:

$$G_{\phi} = \begin{bmatrix} \cos \phi & 0 & -\sin \phi \\ 0 & 1 & 0 \\ \sin \phi & 0 & \cos \phi \end{bmatrix} \quad G_{\psi} = \begin{bmatrix} 1 & 0 & 0 \\ 0 & \cos \psi & \sin \psi \\ 0 & -\sin \psi & \cos \psi \end{bmatrix} \quad G_{\theta} = \begin{bmatrix} \cos \theta & \sin \theta & 0 \\ -\sin \theta & \cos \theta & 0 \\ 0 & 0 & 1 \end{bmatrix} \quad (3)$$

The acceleration due to gravity in the body-fixed frame following a roll, pitch, yaw transformation is thus:

$$\mathbf{g}_{xyz} = G_\phi G_\psi G_\theta \mathbf{g}_{XYZ} \quad (4)$$

where $\mathbf{g}_{xyz} = [g_x \ g_y \ g_z]^T$. The vehicle begins to slip when the traction force is equal to the sum of the centripetal and gravitational force components:

$$|mv^2 \rho + mg_x| = \mu mg_z \quad (5)$$

Note that accelerations other than gravity in the z-direction are ignored. The maximum curvature before slip occurs is given as:

$$\rho_{slip}^{\min, \max} = \frac{-g_x \pm \mu g_z}{v^2} \quad (6)$$

The two solutions correspond to downhill/uphill travel. Let C be defined as the set of allowable vehicle curvatures based on sideslip limits:

$$C(\phi, \psi, \varpi, \mu, v) \equiv \left\{ \forall \rho \mid \rho_{slip}^{\min}(\phi, \psi, \varpi, \mu, v) < \rho < \rho_{slip}^{\max}(\phi, \psi, \varpi, \mu, v) \right\} \quad (7)$$

Roll-over is defined as a vehicle rotation greater than 90 degrees about its longitudinal axis. Potential for roll-over is initiated when the moment about either of the points A in Figure 3 is equal to zero. The maximum curvature before potential roll-over occurs is given as:

$$\rho_{roll-over}^{\max, \min} = \frac{dg_z \pm hg_x}{hv^2} \quad (8)$$

The two solutions correspond to uphill/downhill travel. Let D be defined as the set of admissible curvatures and velocities such that roll-over does not occur:

$$D(\phi, \psi, \varpi, \mu, v) \equiv \left\{ \forall \rho \mid \rho_{roll-over}^{\min}(\phi, \psi, \varpi, \mu, v) < \rho < \rho_{roll-over}^{\max}(\phi, \psi, \varpi, \mu, v) \right\} \quad (9)$$

The ATS is then defined as $N = A \cap B \cap C \cap D$.

Figure 4 shows how the ATS changes as the terrain roll angle increases for a small (0.27 m long) UGV. This example corresponds to a vehicle traversing a side slope with the fall line perpendicular to the vehicle's heading. As expected the vehicle can safely execute downhill turns with greater velocity than it can execute uphill turns, since gravity counters the centripetal acceleration.

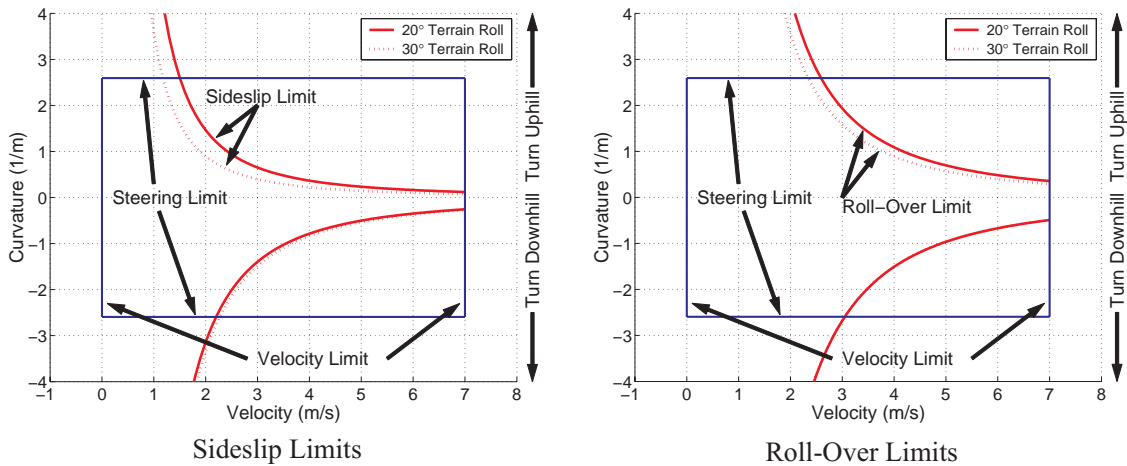


Figure 4: Admissible trajectory space for varying terrain roll angle

Similar results can be observed when the tire/terrain friction coefficient is varied while maintaining a constant roll and pitch angle. In this case a higher traction coefficient allows a UGV to execute sharper turns at a given speed.

4.4 Effect of Hazards on the Trajectory Space

Hazards (obstacles) are defined as discrete objects or terrain features greater than one-half the vehicle wheel radius, such as trees, boulders, ditches, hillocks, and knolls or any area of poorly traversable terrain (i.e. non-geometric hazards such as water or very soft soil). Hazards are represented as “gaps” in the trajectory space. Some obstacles, such as boulders, water traps, and trees disallow a range of curvatures between $\rho_{obstacle}^{\max}$ and $\rho_{obstacle}^{\min}$ respectively, from the current UGV position (see Figure 5). Curvatures between $\rho_{obstacle}^{\max}$ and $\rho_{obstacle}^{\min}$ belong to the obstacle space, E . If a UGV maintains a curvature that lies in E , the UGV will collide with the obstacle.

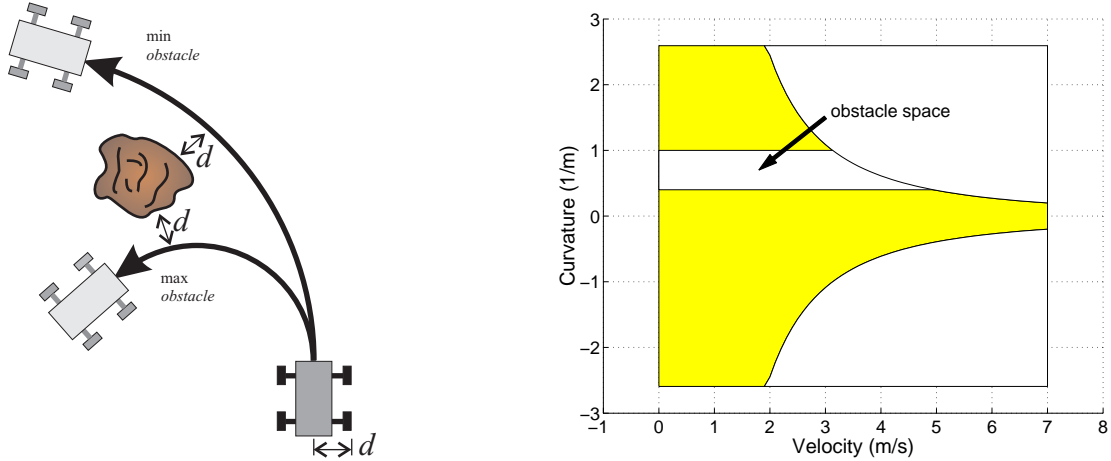


Figure 5: Admissible trajectory space with obstacle.

Other obstacles such as ditches and knolls do not have associated curvatures. Instead they have associated minimum and maximum velocities, $v_{obstacle}^{\min}$ and $v_{obstacle}^{\max}$, respectively. An example would be a ditch that can be traversed ballistically at high speeds, but would cause entrapment at low speeds. Let the obstacle space be defined as:

$$E \equiv \left\{ \forall (v, \rho) \mid v_{obstacle}^{\min} \leq v \leq v_{obstacle}^{\max}, \rho_{obstacle}^{\min} \leq \rho \leq \rho_{obstacle}^{\max} \right\} \quad (10)$$

The modified ATS is $N = (A \cap B \cap C \cap D) - E$.

4.5 Effect of Terrain Roughness on the Trajectory Space

UGV dynamic performance over smooth, well-characterized terrain can be modeled and predicted to a relatively high degree of certainty.^{14,15} However, in rough terrain it is difficult to accurately model complex phenomena such as sideslip, ballistic motion, and wheel/terrain interaction. Compounding these issues is the fact that vehicle parameters may be time-varying due to UGV fuel consumption and payload changes. To overcome these difficulties a Monte Carlo method for predicting vehicle performance has been developed.^{14,15} The approach relies on the observation that although robot and terrain parameters are often not precisely known, the uncertainty associated with these parameters can usually be estimated. A summary of the analysis methodology is as follows:

1. Define vectors of the mean values $\bar{x}_{in} \in \mathcal{R}^p$ and corresponding standard deviations $\sigma_{in} \in \mathcal{R}^p$ for all vehicle and terrain model parameters. This is termed the input parameter space. Uncertainty estimates are derived from engineering judgment, and might depend on physical measurement precision, expected environmental variation for a given task, and sensor uncertainty. Further, this uncertainty can be viewed as a measure of model complexity for phenomena that are

measurable but difficult to characterize, such as wheel/terrain interaction. Here we assume a Gaussian distribution for parameter uncertainty.

2. Randomly generate a sample set of parameter values, $\bar{\mathbf{x}}_{in} \in \mathfrak{R}^P$, from the nominal values and their corresponding standard deviations.
3. Define a metric based on task criteria (e.g. stopping distance or path tracking error). Evaluate the model response to the task and record the metric output, \mathbf{y}_{out} .
4. Repeat steps 2 and 3 k times such that the 99% confidence interval on the bounds of \mathbf{y}_{out} converges.

An example of this technique applied to a ditch traversal is shown below. A 15 degree of freedom UGV model that considered vehicle roll, pitch, yaw, suspension dynamics, tire dynamics (including wheel slip), ballistic motion, and a simplified model of wheel-terrain interaction was developed in ADAMS, a commercial dynamic modeling software package. The tires are modeled as deformable and the terrain is modeled as rigid.

A smooth terrain with a ditch three wheel diameters long and one wheel diameter deep was created. Terrain roughness was then overlaid onto this “idealized” terrain. For this case, terrain roughness was generated using a fractal number of 2.1 with a grid spacing of one wheel diameter and height scaling of two wheel diameters.^{11,16} Fifty separate terrains were created in this fashion with the same roughness but variable height scaling (see Figure 6). This variability physically corresponds to uncertainty in terrain elevation that might be a product of range sensor error or uncertainty.

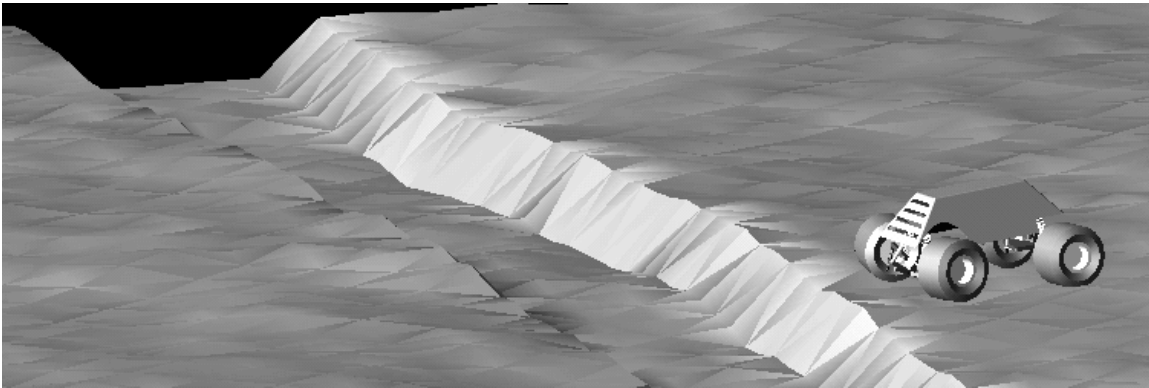


Figure 6: Image of rough terrain ditch traversal simulation. Ditch is three wheel diameters wide, one wheel diameter deep.

A UGV was commanded to traverse each terrain at speeds ranging from 0.4 to 7.6 m/s. The metric \mathbf{y}_{out} was a binary go/no-go measure of successful traversal. For illustration purposes the vehicle and terrain parameters were assumed to be precisely known; only the exact terrain profile was unknown. Figure 7 shows a plot of ditch traversal success probability as a function of speed along with an associated ATS. For “idealized” obstacles (i.e. with no terrain roughness), obstacle traversal success is deterministic (dotted line). For rough terrain, traversal success is probabilistic (solid line). Notice that at low speeds the UGV is able to enter and then climb out of the ditch. At medium speeds the UGV impacts the far wall of the ditch and is stopped. At high speeds the UGV exhibits ballistic behavior and is able to “jump” the ditch. (Note that such a hazard can be termed a velocity-dependent hazard. This type of obstacle is unique to high-speed traversal). The rough-terrain ATS displays a grayscale image corresponding to the probability of safe traversal, with white equaling a zero percent probability of success and black representing a one hundred percent probability.

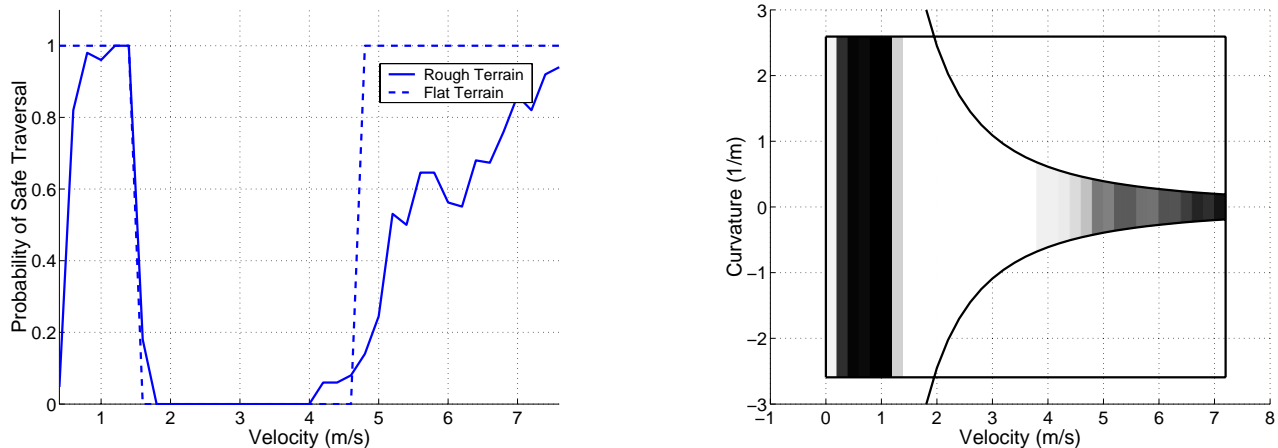


Figure 7: Probability of safe ditch traversal on flat and rough terrain (left) and the associated rough terrain ATS (right).

A second example that shows the effect of rough terrain on UGV roll-over is shown in Figure 8. In this case four terrains were created. The first was flat, smooth terrain. The three other terrains were modeled using a fractal number of 2.5 with one wheel diameter wheel spacing and a height scaling of three to five wheel diameters. The model response metric was the curvature and velocity pair at which the UGV rolls over, shown in Figure 8 for 48 trials.

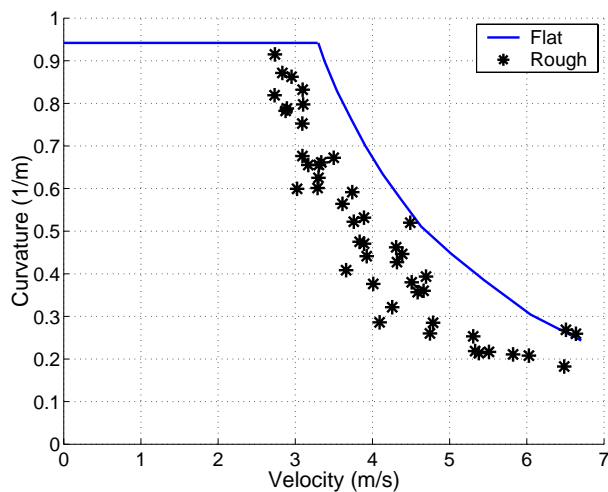


Figure 8: ATS showing roll-over limit on flat, benign, and rough terrain.

In rough terrain the UGV tends to roll-over at lower speeds for a given curvature than when traveling on flat ground. This is due to the dynamic effects that are excited by the interaction of the vehicle's suspension with the rough ground. Such effects would be extremely difficult to reliably predict using deterministic modeling methods, as it would require precise knowledge of the vehicle properties, terrain profile, and vehicle/terrain interaction phenomena. Also notice that the UGV exhibits roll-over at various velocities for the same curvature. This is due to the random nature of the terrain. In summary, the admissible trajectory space is a compact model-based representation of a UGV's performance limits on uneven terrain. It considers the robot's kinematic and dynamic characteristics, steering limits, power train limits, dynamic limits, obstacles, and terrain parameters. The admissible trajectory space is used as the basis for the fast online hazard avoidance algorithm.

5 HIGH-SPEED HAZARD AVOIDANCE

During high-speed navigation, emergency situations (such as negative obstacle detection at short range) are likely to occur that require a UGV to rapidly perform a hazard avoidance maneuver. Two fundamental questions are (1) *when* should a hazard avoidance maneuver be enacted and (2) *which* maneuver should be enacted.

Here we assume a scenario similar to that illustrated in Figure 9. Here a UGV attempts to follow a pre-planned nominal trajectory, $\tau_{nominal} \equiv (v(t), \rho(t))$, which is the output of a high-level path planner. An on-board range sensor measures the terrain elevation in front of the vehicle. The sensor scan is divided into n discrete vehicle-sized patches. The size and number of these patches, sensor accuracy, and throughput are important issues, but are beyond the scope of this paper. The ATS of each patch is computed. Note that these ATSs can be computed offline for a given set of terrain parameters, stored in a library, and then rapidly accessed online.

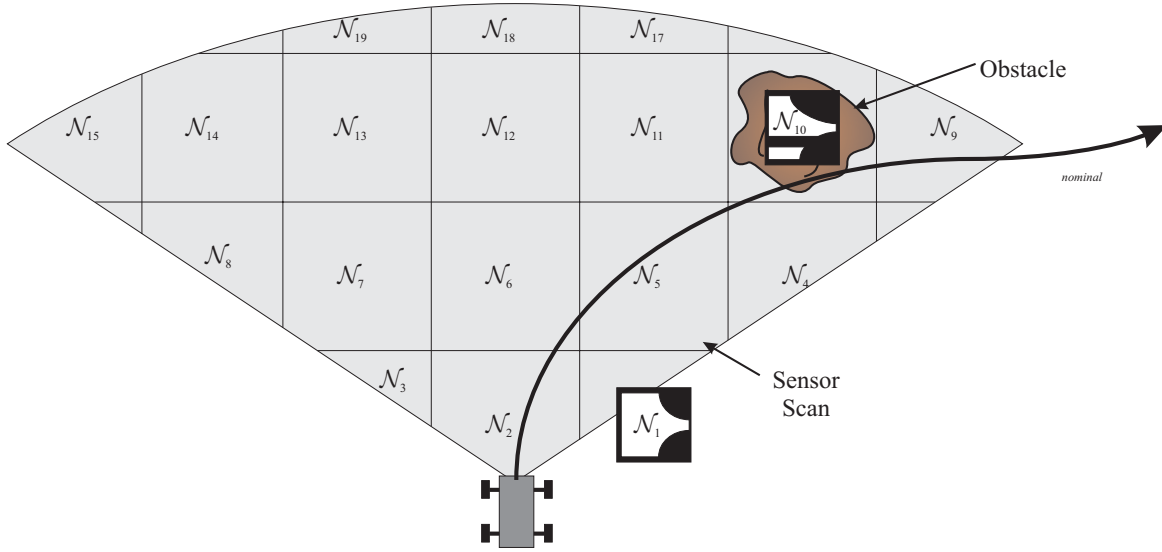


Figure 9: Admissible Trajectory Spaces defined with hazard present.

Let N_i^* denote the ATS for a patch that intersects $\tau_{nominal}$. Let N_{traj} be defined as the intersection of all N_i^* .

$$N_{traj} \equiv N_1^* \cap \dots \cap N_m^* \quad (11)$$

where m is the number of patches that $\tau_{nominal}$ intersects. A maneuver is enacted when an obstacle lies on the vehicle's current desired path or when the desired trajectory will command the vehicle to move outside of the ATS at a future time (i.e. a UGV is given a dynamically inadmissible trajectory on a given terrain). That is, if some element of $\tau_{nominal} \notin N_{traj}$ then enact a hazard avoidance maneuver.

Let the total admissible trajectory space (TATS) be defined as the intersection of all ATSs in the sensor scan:

$$N_{total} \equiv N_1 \cap \dots \cap N_n \quad (12)$$

To determine which maneuver to enact, first let τ_t describe the UGV velocity and curvature at time t . Let $\tau_{t+\Delta t}$ be the UGV velocity and curvature at the time when the UGV would impact the nearest hazard. Note that $\tau_{t+\Delta t} \notin N_{traj}$ and thus $\tau_{t+\Delta t} \notin N_{total}$. The goal of hazard avoidance is to find $\tau^* | \tau^* \in N_{total}$. The maneuver thus transitions the vehicle from a location that lies outside the ATS to one that lies inside.

To find τ^* the trajectory space is discretized into evenly and closely spaced points. Standard search techniques can be used to find a suitable τ^* . In this work we employ a search technique that penalizes decreasing speed and encourages turning such that the absolute value of the curvature approaches zero. The result is a new position inside the ATS that

corresponds to a particular curvature and velocity for hazard avoidance. A low-level control algorithm is then employed to command the UGV to the new curvature and velocity.

6 SIMULATION RESULTS

A simulation was performed of a four wheel independent suspension UGV traveling at 4 m/s over rough terrain with a traction coefficient of 1.0. The vehicle length was 0.27 m and the wheel diameter was 0.12 m. Terrain roughness had a fractal number of 2.05 with a grid spacing of 2 wheel diameters and height scaling of 35 wheel diameters. The resulting distance between the highest and lowest points in the terrain was 14.9 wheel diameters. The nominal speed of 4 m/s was fast enough to excite the suspension dynamics of this small vehicle. This is evident by noting the roll and pitch angles of the vehicle body for a typical traversal as shown in Figure 10.

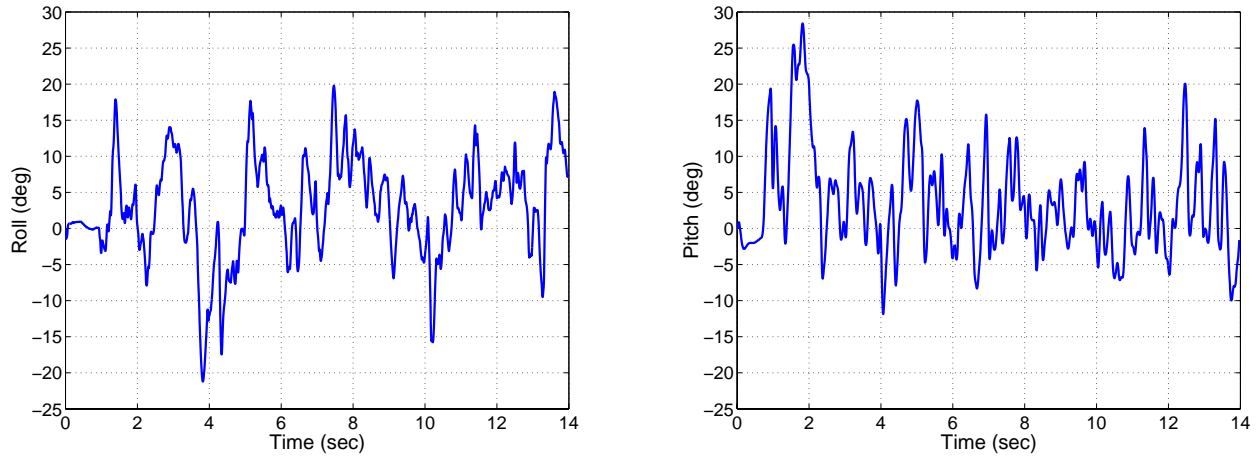


Figure 10: UGV roll and pitch angles.

The dynamic nature of the scenario is also conveyed by wheel slip, defined as:

$$S = 1 - \frac{v}{R_e \omega} \quad (13)$$

where R_e is the effective wheel radius and ω is the wheel angular velocity. Wheel slip for a typical traversal is shown in Figure 11.

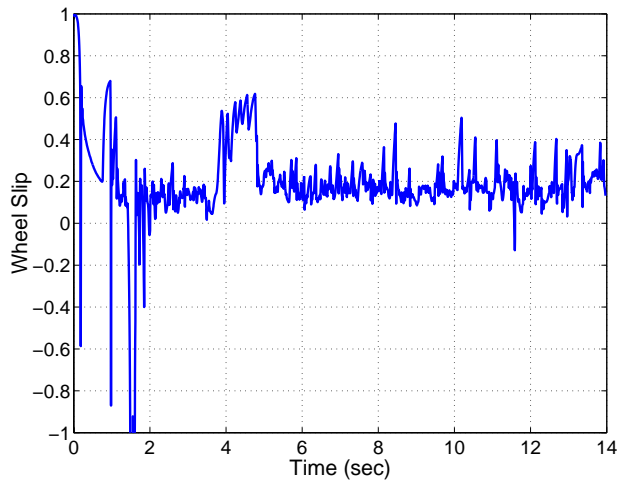


Figure 11: Wheel slip

A sensor range of 20 vehicle lengths (5.4 m) with a field of view of +/- 70 degrees was utilized. It is assumed that multiple range sensors might be used to cover this range. Figure 12 shows simulation results of a vehicle avoiding multiple obstacles using the trajectory space hazard avoidance algorithm. The original path was a straight line from start to finish. Here the original trajectory was resumed once the obstacle was passed. Once the admissible trajectory space was loaded into the computer's memory, the online search for a hazard avoidance maneuver took 276 μ sec using non-optimized Matlab code on a P4 1.5 GHz desktop computer. A complete re-planning algorithm is an area of current research.

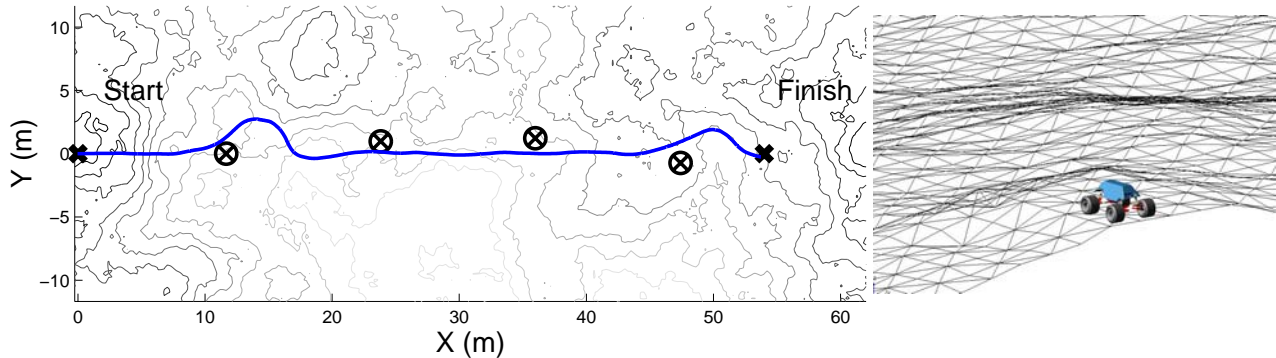


Figure 12: Hazard avoidance simulation results (left). A circled X indicates a hazard location. Hazard sizes are seven wheel diameters (1.45 m) wide. Terrain used in the simulation (right).

7 CONCLUSIONS

This paper has presented a model-based analysis tool and hazard avoidance algorithm for UGVs in rough terrain. The concept of the trajectory space, which captures complex vehicle dynamics over uneven and rough terrain, was developed. The paper briefly described a stochastic analysis methodology that considers parameter uncertainty, and shows how this uncertainty can be incorporated into the trajectory space. The admissible trajectory space was presented, which describes UGV performance limits on uneven terrain. This information was used as the basis of a hazard avoidance algorithm. Future work will focus on the development of a complete re-planning algorithm using the techniques described in this paper.

REFERENCES

-
1. Walker, J. "Unmanned Ground Combat Vehicle Contractors Selected." DARPA News Release February 7, 2001. www.darpa.mil
 2. Gerhart, G., Goetz, R., and Gorsich, D. "Intelligent Mobility for Robotic Vehicles in the Army after Next." Proceedings of the SPIE Conference on Unmanned Ground Vehicle Technology, 3693 (1999).
 3. Coombs, D., et al. "Driving Autonomously Off-road up to 35 km/h." Proceedings of the IEEE Intelligent Vehicle Symposium 2000 (2000): 186-191.
 4. Daily, M. et al. "Autonomous Cross-Country Navigation with the ALV." Proceedings of the IEEE International Conference on Robotics and Automation 2 (1988): 718-726.
 5. Olin, K. Tseng, D. "Autonomous Cross-Country Navigation: An Integrated Perception and Planning System." IEEE Expert 6.4 (1991): 16- 30
 6. Kelly, A., and Stentz, A. "Rough Terrain Autonomous Mobility – Part 1: A Theoretical Analysis of Requirements." Autonomous Robots 5 (1998): 129-161.

-
7. Laugier, C. et al. "Sensor-Based Control Architecture for a Car-Like Vehicle." Proceedings of the IEEE International Conference on Robotics and Automation (1998): 216-222.
 8. Langer, D., Rosenblatt, J.K., and Hebert, M. "A Behavior-Based System for Off-Road Navigation." IEEE Transactions of Robotic and Automation 10.6 (1994): 776-783.
 9. Urmson, C. "Locally Randomized Kinodynamic Motion Planning for Robots in Extreme Terrain." Ph.D. Thesis Proposal, The Robotics Institute Carnegie Mellon University (2002).
 10. Frazzoli, E., Dahleh, M., and Feron, E. "Robust Hybrid Control for Autonomous Vehicle Motion Planning." Proceedings of the 39th IEEE Conference on Decision and Control 1 (2000): 821-826.
 11. Dudgeon, J. and Gopalakrishnan, R. "Fractal-Based Modeling of 3D Terrain Surfaces." Proceedings of the IEEE Conference on Bringing Together Education, Science, and Technology, (1996): 246-252.
 12. Iagnemma, K., and Dubowsky, S. Estimation, Motion Planning, and Control of Mobile Robots in Rough Terrain with application to Planetary Rovers. STAR Series on Advanced Robotics, Springer, 2004.
 13. Iagnemma, K., Kang, S., Brooks, C., Dubowsky, S. "Multi-Sensor Terrain Estimation for Planetary Rovers." Proceedings of the 7th International Symposium on Artificial Intelligence, Robotics, and Automation in Space, i-SAIRAS, (2003).
 14. Golda, D. Modeling and Analysis of High-Speed Mobile Robots Operating on Rough Terrain. M.S. Thesis, Massachusetts Institute of Technology, 2003.
 15. Golda, D., Iagnemma, K., and Dubowsky, S. "Probabilistic Modeling and Analysis of High-Speed Rough-Terrain Mobile Robots." 2004 IEEE International Conference on Robotics and Automation, (submitted).
 16. Mandelbrot, B. B. The Fractal Geometry of Nature. Freeman and Company, 1977.